

See discussions, stats, and author profiles for this publication at:  
<https://www.researchgate.net/publication/256148159>

# Theoretical study on the geometry dependence of the second hyperpolarizability of the allyl cation based on a numerical Liouville three-type analysis

ARTICLE *in* CHEMICAL PHYSICS LETTERS · MARCH 1996

Impact Factor: 1.9 · DOI: 10.1016/0009-2614(96)00109-1

---

CITATIONS

14

---

READS

4

4 AUTHORS, INCLUDING:



Masayoshi Nakano

Osaka University

337 PUBLICATIONS 4,769 CITATIONS

SEE PROFILE

# Theoretical study on the geometry dependence of the second hyperpolarizability of the allyl cation based on a numerical Liouville three-type analysis

Masayoshi Nakano, Satoru Yamada, Isamu Shigemoto, Kizashi Yamaguchi

*Department of Chemistry, Faculty of Science, Osaka University, Toyonaka, Osaka 560, Japan*

Received 30 January 1995; in final form 17 January 1996

---

## Abstract

The second hyperpolarizability ( $\gamma$ ) of the allyl cation is analyzed in terms of the virtual excitation processes by the numerical Liouville approach (NLA). The influence of molecular geometry on  $\gamma$  is investigated. The results indicate that molecular geometry affects the magnitude and sign of  $\gamma$  and that three types of virtual excitation process exhibit remarkably different dependence on the molecular geometry. A negative  $\gamma$  for  $C_{2v}$  geometry without bond alternation is shown to be converted to a positive  $\gamma$  for bond-alternated geometry. Implications of the results are discussed in relation to a polymeric system with a charged defect.

---

## 1. Introduction

Investigations of molecular (hyper)polarizability are important in studies of non-linear optical phenomena [1–3]. Many theoretical approaches based on the ab initio and semi-empirical molecular orbital (MO) methods have been applied to the elucidation of the mechanism of molecular non-linear optical responses [3]. In our previous papers [4–6] we discussed the relationship between the second hyperpolarizability ( $\gamma$ ) and molecular electronic states and symmetry, and we classified  $\gamma$  based on the contributing virtual excitation processes. This classification has shown that third-order non-linear optical processes involve both positive and negative contributions. In general, almost all organic molecules are known to exhibit positive  $\gamma$ s in the off-resonant region. However, this classification of  $\gamma$  predicts the existence of systems with negative  $\gamma$  for centrosym-

metric systems, where the polarizability ( $\alpha$ ) for the ground state is larger than that in the first excited state. Systems with negative  $\gamma$  are important in quantum optics since negative  $\gamma$  causes a self-defocusing effect. Therefore, we examined various types of electronic states of centrosymmetric alternant and condensed-ring conjugated systems as candidate for a system with negative  $\gamma$ , and found that the radical cation states of certain condensed-ring conjugated systems exhibit large negative  $\gamma$ s [7].

On the other hand, it has been pointed out that variations in molecular geometry can reverse the sign of  $\gamma$ . For example, Melo et al. [8] reported that regular polyenes possess positive longitudinal  $\gamma$ s, while small-size charged soliton-like polyenes exhibit large negative  $\gamma$ s. Therefore, we take the allyl cation molecule in the present study as one of the simplest model systems with a charged defect in order to elucidate the relationship between the de-

gree of C–C bond-length alternation and  $\gamma$ , which has been predicted to be negative in the equilibrium geometry by ab initio coupled-cluster (CC) calculations [7]. Virtual excitation processes are analyzed in the numerical Liouville approach (NLA) [9–11]. We also discuss the variations in the contributions from three types of virtual excitation processes with respect to the bond-length alternation.

## 2. Calculation method and molecular geometry

Fig. 1 shows the molecular geometry of the allyl cation optimized by using the ab initio Hartree–Fock (HF) method with the 6-31G\*\* basis set. The C–C bond-length alternation, denoted by  $\Delta r = l(C_1-C_2) - l(C_2-C_3)$ , is varied by shifting the middle carbon  $C_2$  along the  $z$  axis, as shown by a thick arrow.

We apply the NLA to the calculation of the off-resonant  $\gamma$  in third-harmonic generation (THG). The NLA is based on a numerical Fourier transformation of the time series of polarization obtained by using numerical solutions of the quantum Liouville equation. This approach can provide numerically exact on- and off-resonant hyperpolarizabilities including population and phase relaxation effects. To apply the NLA, we first construct a state model that mimics the electronic states of the system and calculate its transition energies and transition moments. As shown by previous ab initio finite-field (FF) calculations [7], the hyperpolarizability of the allyl cation is found to be primarily contributed by virtual excitation processes involving the  $\pi$ -electron excited states and is much influenced by  $\pi$ -electron correlations. Therefore, only  $\pi$ -electron excited states are

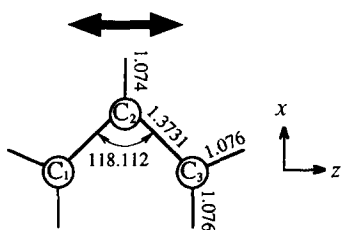


Fig. 1. Structures of the allyl cation optimized by ab initio HF method using the 6-31G\*\* basis set. Bond lengths (Å) and bond angles (°) are shown. A thick arrow indicates the shift of the middle carbon.

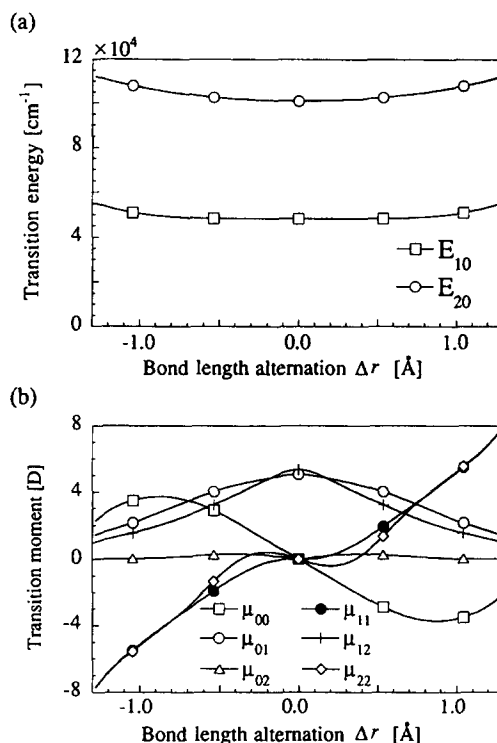


Fig. 2. (a) Variations in transition energies,  $E_{ij} (= E_i - E_j)$  ( $\text{cm}^{-1}$ ), and (b) transition moments,  $\mu_{ij}$  (D), of a three-state model. The power density is  $100 \text{ MW}/\text{cm}^2$  and the frequency of the external fields is  $10000 \text{ cm}^{-1}$ .

considered in our  $N$ -state model. In general, quantitative prediction of the transition properties (transition energies and transition moments) should be performed by an ab initio large-scale CI calculation using extended basis sets augmented by polarization and diffuse functions. However, the main purpose of this study is to obtain qualitative results of the molecular geometry dependence of the  $\gamma$ s; therefore, the transition properties related to the  $\pi$ -electron excited states are calculated using semi-empirical INDO/S with single and double excitation configuration interactions (SDCI) [12] (using all  $\pi$  electrons), the method of which has been proven to reproduce reliable transition properties of organic molecules at a much lower cost than large-scale ab initio CI. Fig. 2 shows the transition energies and transition moments of the three-state model calculated by the INDO/S-SDCI method for  $\Delta r = -1.3$  to  $1.3 \text{ Å}$ . We investigate the off-resonant THG pro-

cesses induced by three incident beams with a power density of 100 MW/cm<sup>2</sup>, which is a typical value for non-linear optical effects [9], and a frequency of 10000 cm<sup>-1</sup>, which corresponds to the off-resonant value with respect to the first excited state 1.

### 3. Three-type analysis of virtual excitation processes

Usually, the physical meaning of hyperpolarizability can be understood in terms of the contributing virtual excitation processes. The formula for static  $\gamma$ , Eq. (1), obtained by perturbation theory can be partitioned into three types of virtual excitation processes [6,9–11,13]:

$$\gamma(0) = \sum_n \frac{(\mu_{n0})^2 (\Delta\mu_{n0})^2}{E_{n0}^3} - \sum_{n,m} \frac{(\mu_{n0})^2 (\mu_{m0})^2}{E_{n0} E_{m0}^2} \\ \times \left( \sum_{n' \neq m} \frac{\mu_{0n} \Delta\mu_{n0} \mu_{nm} \mu_{m0}}{E_{n0}^2 E_{m0}} \right. \\ \left. + \sum_{n' \neq m \neq n} \frac{\mu_{0n} \mu_{nm} \mu_{m'n'} \mu_{n'0}}{E_{n0} E_{m0} E_{n'0}} \right), \quad (1)$$

where  $\mu_{ij}$  is the transition moment between states  $i$  and  $j$ ,  $\Delta\mu_{i0}$  is the difference in dipole moments of states  $i$  and 0 (the ground state), and  $E_{i0}$  is the transition energy between states  $i$  and 0. A virtual excitation process in the fourth-order optical process is represented by  $(0-i-j-k-0)$ . The first, the second and third terms on the right-hand side of Eq. (1) correspond to type (I)  $(0-n-n-n-0)$ , type (II)  $(0-n-0-m-0)$  and type (III) contributions, respectively. The type (III) terms can be partitioned into two contributions specified by type (III-1)  $(0-n-n-m-0)$  and type (III-2)  $(0-n-m-n'-0)$ , as illustrated in Fig. 3.

The type (I)  $(0-n-n-n-0)$  process, which involves two dipole moment differences between the

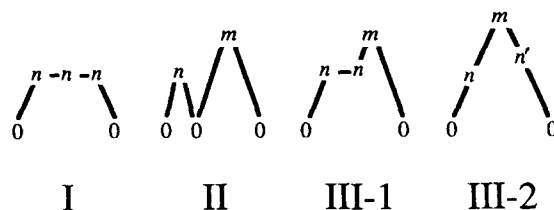


Fig. 3. Schematic diagrams describing the virtual excitation processes which contribute to the second hyperpolarizability  $\gamma$ .

excited ( $n$ ) and ground (0) states ( $\Delta\mu_{n0}$ ) on a virtual excitation path, exists only for molecules with non-centrosymmetric charge distributions.

The type (II)  $(0-n-0-m-0)$  process involves the ground state in the middle of a virtual excitation path. This is negative in the off-resonant region, as shown in Eq. (1).

The type (III-1) process, which involves only one dipole moment difference ( $\Delta\mu_{n0}$ ) on a virtual excitation path, exists only for molecules with non-centrosymmetric charge distributions. In contrast, the type (III-2) process (including the case of  $n = n'$ ), which has no dipole moment difference on a virtual excitation path, can contribute to the  $\gamma$ s of any molecule. The type (III) contributions can have a positive or negative value. Thus, the magnitude and sign of the total hyperpolarizability is shown to be closely related to each virtual excitation process.

The total  $\gamma$  can be partitioned into three types of virtual excitation processes by using the three-type analysis method of the NLA. This analysis is realized by considering several types of sub-model systems, whose transition properties are chosen appropriately. The details of this calculation procedure have been discussed elsewhere [11].

Table 1 gives the various virtual excitation processes involved in the three-type virtual excitation processes for the three-state model of allyl cation with an arbitrary  $\Delta r$ . The type (I) and (III-1) contributions vanish at  $\Delta r = 0$ , but they are non-zero at

Table 1  
Virtual excitation processes classified into three types of processes (I)–(III) for a three-state model system of the allyl cation<sup>a</sup>

(I)	(II)	(III-1)	(III-2)
(Ia) $(0-1-1-1-0)$	(IIa) $(0-1-0-1-0)$	(III-1a) $(0-1-1-2-0)$	(III-2a) $(0-1-2-1-0)$
(Ib) $(0-2-2-2-0)$	(IIb) $(0-2-0-2-0)$	(III-1b) $(0-2-2-1-0)$	(III-2b) $(0-2-1-2-0)$
	(IIc) $(0-1-0-2-0)$		

<sup>a</sup> See Figs. 1 and 3.

$\Delta r \neq 0$  because of the pronounced dipole moment differences between the ground and excited states.

#### 4. Dependence of $\gamma$ of the allyl cation on $\Delta r$

Fig. 4a shows the individual and total types of contributions of the real parts of THG  $\gamma_{zzzz}$  (referred to as  $\gamma$ , subsequently) of the allyl cation with respect

to  $\Delta r$ . The ground-state geometry based on the ab initio HF calculation predicts  $\Delta r = 0$ . In this case, the total  $\gamma$  is observed to be largely negative. In contrast,  $\gamma$  increases remarkably with  $|\Delta r|$ , passes 0, and exhibits a peak in a positive region around  $|\Delta r| = 0.8 \text{ \AA}$ . For  $|\Delta r|$  values larger than  $0.8 \text{ \AA}$ ,  $\gamma$  decreases again. This behavior is found to be similar to that of neutral polyenes end-capped by an acceptor and a donor [14].

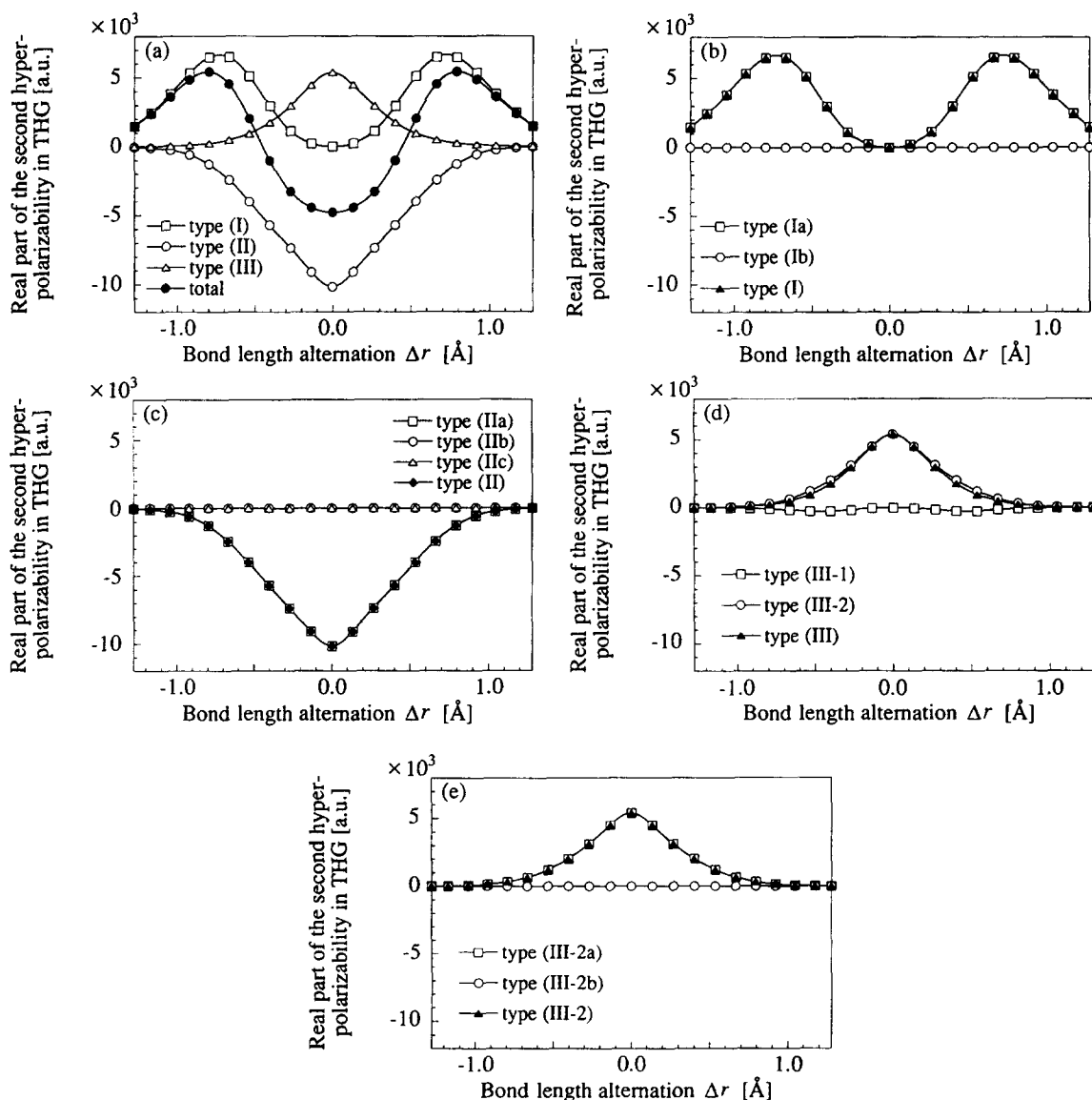


Fig. 4. Real part of the off-resonant second hyperpolarizability  $\gamma$  in THG with respect to the C–C bond-length alternation  $\Delta r$  ( $\text{\AA}$ ): (a) the total  $\gamma$  of type (I)–(III) contributions and (b)–(e) contributions from component types.

As can be seen from Fig. 4a, the type (I) process is a main contribution in the region of large  $|\Delta r|$  ( $\geq 0.8$  Å), while the type (II) and (III) contributions are enhanced around  $|\Delta r| = 0$ . This is considered to be caused by the fact that the molecule with large  $|\Delta r|$  induces large non-symmetric charge distributions (in the direction of the  $z$  axis) which contribute to the type (I) process predominantly, while the molecule around  $\Delta r = 0$  has nearly symmetric charge distributions in the direction of the  $z$  axis, where the type (I) contribution vanishes. For allyl cation, the [type (II)] value outweighs the [type (III)] value, so that the total  $\gamma$  in the region with small  $\Delta r$  turns to be negative.

Fig. 4b shows the variations in type (I), (Ia) and (Ib) contributions with respect to  $\Delta r$ . This figure indicates that the type (I) contribution is almost determined by the type (Ia) process, which is characterized by a large dipole moment difference between the 1 and 0 states. This suggests that the excited state 1 is a charge-transfer (CT) state, which is mainly constructed from single excitation configurations.

Variations in each contribution from the type (II) process [(IIa)–(IIc)] with respect to  $\Delta r$  are shown in Fig. 4c. Apparently, the type (IIa) contribution is essential. This contribution takes the largest absolute value near  $\Delta r = 0$ . As a result, this contribution primarily leads to a large negative  $\gamma$  value of the allyl cation in the equilibrium geometry.

The behavior of the type (III) process is almost determined by that of the type (III-2) process, as shown in Fig. 4d. This contribution consists of the type (III-2a) and (III-2b) processes shown in Fig. 4e. The type (III) contributions are essentially determined by the type (III-2a) process, which is constructed from the virtual excitation process through excited states higher than those involved in the type (Ia) and (IIa) processes.

From the above analysis, it is concluded that  $\gamma$  of the allyl cation at large  $\Delta r$  is dominated by the type (Ia) process, while the total  $\gamma$  at small  $\Delta r$  can be qualitatively described by the type (IIa) and (III-2a) processes. For the allyl cation, the type (IIa) process provides a larger  $|\gamma|$  than the type (III-2a) process, so that the total  $\gamma$  turns out to be negative in the equilibrium geometry.

In summary, the characteristics of the (hyper)polarizability can be interpreted by the inher-

ent quantum (virtual excitation) processes, which can be modified by the variations in the conformation and charged states. For example, a negative  $\gamma$  for the allyl cation in the equilibrium geometry implies that the contributing virtual excitations tend to be limited to the low-lying virtual excitation process (0–1–0–1–0). This strong low-lying excitation process seems to be attributed to the charged defect in the allyl cation. Similar tendencies seem to exist in charged soliton-like polyenes with small chain lengths [8]. In contrast, in the region remote from the equilibrium geometry a large positive contribution to  $\gamma$  is dominated by the virtual excitation process (0–1–1–1–0), which represents the virtual CT in the molecule with non-symmetric charge distributions in the ground state.

## 5. Concluding remarks

We have made an NLA three-type analysis of the virtual excitation processes of  $\gamma$  of a three-state model system which mimics the electronic states of the allyl cation. This system is found to exhibit a pronounced negative  $\gamma$  in the equilibrium geometry due to the large contribution of the type (IIa) (0–1–0–1–0) process involving strong virtual excitations between the ground state and first allowed excited state 1. This suggests that the charged defect in the allyl cation tends to enhance the contributions from the virtual excitations between the first allowed excited (1) and the ground (0) states rather than the type (III) contributions which involve virtual excitation paths passing through high-lying excited states. It is further predicted that the introduction of a charged defect into a small-size regular polymeric chain causes the inversion of the sign of  $\gamma$  of the chain because of the enhancement of the type (II) (0– $n$ –0– $n$ –0) contribution larger than that of the type (III-2) (0– $n$ – $m$ – $n$ –0) contribution. This analysis provides a qualitative explanation of the negative  $\gamma$  of the charged soliton-like small-size polyene calculated by Melo et al. [8].

Calculation of the allyl cation with large bond-length alternation is found to yield a positive total  $\gamma$ . This is caused by the type (Ia) (0–1–1–1–0) process, which is related to a large dipole moment difference between the ground (0) and the first CT excited (1) states. Therefore, the bond-length alterna-

tion tends to cause non-symmetric charge distributions, which are closely related to the strong virtual CT in the molecule.

As mentioned above, the second hyperpolarizability  $\gamma$  exhibits a strong dependence on its nuclear conformation. This suggests that, in the presence of the influence of solvent molecules and the dielectric medium, variations in molecular geometries can induce significant variations in the sign and magnitude of  $\gamma$ . Furthermore, nuclear motions are also expected to affect the hyperpolarizabilities of highly polarizable molecules.

### Acknowledgements

We are grateful to the Ministry of Education, Science and Culture of Japan (Specially Promoted Research No. 06101004) for financial support.

### References

- [1] D.P. Craig and T. Thirunamachandran, *Molecular quantum electrodynamics* (Academic Press, New York, 1984).
- [2] N. Bloembergen, *Nonlinear optics* (Benjamin, New York, 1965).
- [3] P.N. Prasad and D.J. Williams, *Introduction to nonlinear optical effects in molecules and polymers* (Wiley, New York, 1990).
- [4] M. Nakano, I. Shigemoto, S. Yamada and K. Yamaguchi, *J. Chem. Phys.* 103 (1995) 4175.
- [5] M. Nakano, K. Yamaguchi and T. Fueno, *Synth. Metals* 41–43 (1991) 3755.
- [6] M. Nakano and K. Yamaguchi, *Chem. Phys. Letters* 206 (1993) 285.
- [7] M. Nakano and K. Yamaguchi, *Mol. Cryst. Liq. Cryst. A* 255 (1994) 139.
- [8] C.P. de Melo and R. Silbey, *J. Chem. Phys.* 88 (1988) 2567.
- [9] M. Nakano and K. Yamaguchi, *Phys. Rev. A* 50 (1994) 2989.
- [10] M. Nakano, K. Yamaguchi, Y. Matsuzaki, K. Tanaka and T. Yamabe, *Chem. Phys. Letters* 233 (1995) 411.
- [11] M. Nakano, K. Yamaguchi, Y. Matsuzaki, K. Tanaka and T. Yamabe, *J. Chem. Phys.* 102 (1995) 2996.
- [12] A.D. Bacon and M.C. Zerner, *Theoret. Chim. Acta* 53 (1979) 21.
- [13] M. Nakano, M. Okumura, K. Yamaguchi and T. Fueno, *Mol. Cryst. Liq. Cryst. A* 182 (1990) 1.
- [14] S.R. Marder, C.B. Gorman, F. Meyers, J.W. Perry, G. Bourhill, J.L. Bredas and B.M. Pierce, *Science* 265 (1994) 632.